

# The impact of turbulence intensity and atmospheric stability on power deficits due to wind turbine wakes at Horns Rev wind farm

**Hansen, Kurt Schaldemose; Barthelmie, Rebecca J.; Jensen, Leo E.; Sommer, Anders**

*Published in:*
Wind Energy

*Link to article, DOI:*
10.1002/we.512

*Publication date:*
2012

# The impact of turbulence intensity and atmospheric stability on power deficits due to wind turbine wakes at Horns Rev wind farm

Kurt S. Hansen[1]
Department of Mechanical Engineering, Technical University of Denmark,
ksh@mek.dtu.dk

Rebecca J. Barthelmie[2],
Atmospheric Science and Sustainability
Indiana University
Bloomington
IN 47405
rbarthel@indiana.edu

Leo E. Jensen[3]
DONG Energy A/S,
7000 Fredericia,
Denmark
LEOJE@dongenergy.dk

Anders Sommer[4]
Vattenfall AB,
7000 Fredericia,
Denmark
Anders.Sommer@vattenfall.com

## Abstract

The wind turbine operational characteristics, power measurements and the meteorological measurements from Horns Rev offshore wind farm have been identified, synchronized, quality screened and stored in a common database as 10 minute statistical data. A number of flow cases have been identified to describe the flow inside the wind farm and the power deficits along rows of wind turbines have been determined for different inflow directions and wind speed intervals. A method to classify the atmospheric stability based on the Bulk-Ri number has been implemented. Long term stability conditions have been established that confirm, in line with previous results, that conditions tend towards near-neutral as wind speeds increase but that both stable and unstable conditions are present at wind speeds up to 15 $ms^{-1}$. Moreover, there is a strong stability directional dependence with southerly winds having fewer unstable conditions while northerly winds have fewer observations in the stable classes. Stable conditions also tend to be associated with lower levels of turbulence intensity and this relationship persists as wind speeds increase. Power deficit is a function of ambient turbulence intensity. The level of power deficit is strongly dependent on the wind turbine spacing and as turbulence intensity increases the power deficit decreases. The power deficit is determined for four different wind turbine spacing distances and for stability classified as very stable, unstable and other (near-neutral to very unstable). The more stable conditions are, the larger the power deficit.

**Keywords**: wind farms, offshore, stability, wakes, observations, power deficits.

## 1 Introduction

As wind farms increase in size a fundamental issue with accurately estimating power output has been noted and may be due in part to modeling flow and wakes [1]. Wind turbine wakes

are complex and their relationship with atmospheric variables such as the variability of wind speed, wind direction, turbulence intensity and atmospheric stability is not yet fully understood (see e.g. [1], [2]), particularly for large arrays where the modification of the flow appears to occur on a number of spatial scales [3]. In order to improve wind farm and wake models, further understanding of the relationships between wakes and the atmosphere are required.

A detailed analysis of the atmospheric conditions and the flow deficit due to wind farm wakes have been investigated inside the Horns Rev offshore wind farm in Denmark as part of two EU funded research projects. Preliminary analysis of wake measurements at Horns Rev wind farm were reported in [4] and in [5], an estimate of total wind farm efficiency of about 90% was given and the importance of atmospheric stability in determining wind turbine wake losses was stated. Recent release of two years additional data have increased the database size and enabled an examination of wakes with a higher resolution in terms of wind speed, wind direction, turbulence intensity and stability. While stable conditions can persist at high wind speeds, high wind speeds tend to force conditions towards neutral, at least in northern European waters [6], [7]. Despite the limited number of datasets, the impact of turbulence intensity and stability on wind turbine wakes has been examined previously. For offshore wind farms, velocity deficits tend to be larger in stable than in near-neutral conditions [3], [5], [8] and wake recovery tends to be slower. The relationship between wind speed, turbulence intensity and atmospheric stability offshore is somewhat complex. Turbulence intensity at turbine heights (above 50 m) is typically less than 6% offshore and has been shown to be high at low wind speeds and at high wind speeds with a minimum between 8 and 12 $ms^{-1}$ [8], [9]. This implies that for wind speeds in the frequently occurring range of 8-12 $ms^{-1}$, where wake losses are relatively high due to high thrust coefficients, turbulence intensity can be relatively low impacting wake recovery at these wind speeds. Conversely, at lower wind speeds when turbines are still operating (4-8 $ms^{-1}$) turbulence intensity may be higher at hub-height depending on stability conditions. Recent analysis has been initiated to evaluate the impacts of atmospheric stability and turbine spacing on the magnitude of the power deficit induced by wind turbine [3].

## 2 Wind farm layout

The Horns Rev wind farm (HR) has a shared ownership by Vattenfall AB (60%) and DONG Energy AS (40%). It is located 14 km from the west coast of Denmark as shown in Figure 1b,

with a water depth of 6-14 m. The wind farm has a rated capacity of 160 MW comprising 80 wind turbines, which are arranged in a regular array of 8 by 10 turbines. The wind turbines are installed with an internal spacing along the main directions of 7 D, as shown in Figure 1a. The diagonal wind turbine spacing is either 9.4 D or 10.4 D. Figure 1a furthermore illustrates the location of the three offshore meteorological masts associated with the wind farm. Mast M2, with a height of 62m, was installed prior to the wind farm installation to document the wind conditions [10]. Two identical masts M6 and M7 were installed as part of the Horns Rev wind farm wake measurements program [11] with a height equal to the hub height. The lowest cup anemometer level is 15 m at M2 and 20 m at M6 and M7.

This analysis includes two periods each of three years; where the first period represents three years of measurements originally used for site assessment 15 May 1999 – 14 May 2002 and the second period represents three years of wind turbine operation 1 Jan 2005 – 31 Dec 2007.

## 2.1 Meteorological measurements

The Horns Rev measurement systems have been in operation for several years and not all instruments have been calibrated or quality controlled regularly. This means that signal quality control has been necessary and some of the procedures presented in [12] have been implemented in this project. Below is a summary of potential problems or uncertainties related to the instruments and observations.

Mast M2, height 62m: The instrumentation consists of Risø high quality cup anemometers combined with ED-vanes and has been in operation since 1999 with regular calibration and inspections, unfortunately the signal quality has decreased during the recent years and the data acquisition system was stopped completely at the beginning of 2007. Furthermore, periods of wind direction measurements were erroneous from 2005 to 2007, which has resulted in a lack of reliable wind direction measurements from mast M2.

Mast M6, height 70m: The instrumentation consists of Risø high quality cup anemometers combined with ED-vanes and has been in operation since 2004 with regular calibration and inspections.

Mast M7, height 70m: The instrumentation consists of Risø high quality cup anemometers combined with ED-vanes and has been in operation since 2004 with regular calibration and inspections.

## 2.2 Wind turbines

The wind farm comprises VESTAS V80 turbines, which are 2 MW pitch controlled, variable speed wind turbines with a diameter of 80 m and 70 m hub height. A limited number of channels have been extracted from the wind farm SCADA system[1] and used to investigate the wind farm flow conditions in combination with the [external] meteorological observations. From each wind turbine, the following data are used to describe the wind turbine operational conditions: Electrical power, rotor speed, pitch angle, yaw position, yaw misalignment and nacelle wind speed, registered as 10 minute statistical values. The SCADA signals are supervised as part of the ordinary wind turbine supervision, but no reports were provided on the SCADA signal quality.

Figure 2 illustrates how the wind turbine operational characteristics in terms of power, thrust, pitch and rotor speed are highly dependent on the local wind speed. The manufacturer's power[2] curve and thrust coefficient[3] curve as function of wind speed are shown in Figure 2a. The combined rotor speed and pitch control are used to obtain a constant thrust coefficient of 0.8 for the wind speed range 4-10 $ms^{-1}$ as shown in Figure 2b. The thrust coefficient decreases for increasing wind speeds. The operational wind turbine characteristic in terms of rotor speed and pitch angle depends on local wind speed, turbulence, wind direction, stability and spacing in the wind farm and are shown in Figure 2b. Wind turbines operating in wake conditions operate at 10-15% lower rotor speeds up to rated power.

## 2.3 Quality of measurements

The meteorological measurements were recorded with stand-alone data acquisition systems and afterwards merged with the SCADA data. Since the data quality was not reported by the data providers, it was necessary to perform quality screening of all data. The contents of this data quality screening with reference to the signal types are listed in [11] and summarized below:

---

[1] Supervisory Control And Data Acquisition [SCADA] system

[2] The official power curve is measured with reference to the IEC 61400-12 Power performance measurements and used in WAsP®.

[3] The thrust coefficient curve is calculated and provided by VESTAS A/S.

1) All wind speed observations from the masts have been controlled for spikes, drop-out and correlated to other heights according to the procedures presented in [11]. Erroneous observations were marked for exclusion.

2) All wind directional observations from the masts have been controlled and correlated with other heights. Erroneous observations were marked for exclusion.

3) All power values have been verified in relation to the nacelle wind speed for each wind turbine and erroneous values were marked. This verification is used to identify observations where the wind turbine was grid connected for the entire duration of the observation. Unfortunately the nacelle wind speed cannot be used to verify the power curves due to lack of calibration of the nacelle anemometer.

4) Power curves for wind turbines wt01, wt05 and wt07 were evaluated[4] with reference to the wind speed recorded at M2, level 62 m - for a free stream (western) direction sector.

5) Power curves for wind turbine wt95 and wt97 were evaluated[4] with reference to the wind speed recorded at M6, level 70 m for a free stream (eastern) sector.

6) The yaw position offset for wt07 has been derived from the wt17 / wt07 power ratio as function of wind direction. Unfortunately all wind turbine yaw position signals have a lack of calibration. wt07 was selected as a reference wind turbine for westerly wind directions (270±65°).

Only five representative power curves have been evaluated and showed a 2-3% deviation[4] from the from the official power curve. Further evaluation of wind turbine power curves at the site is not possible due to a lack of free stream hub-height wind speeds and valid air density measurements. The power curve determined for wind turbine wt07 has been used as a reference power curve in the wake flow analysis. All of the wake analysis presented here that requires free stream wind speed and direction is focused on the westerly sector, except when the analysis is based on measured turbulence intensity. The large distance between the wind farm and mast M2 together with the lack of free stream wind speed measurements means that wake analysis required the use of data from an undisturbed reference wind turbine. The power signal from wt07 combined with the representative power curve for wind turbine wt07 was

[4] The power curve validation is performed without air density correction and with 1.5-5 km separation between wt and mast.

used to establish the free stream wind speed for a western direction sector. The wind speed uncertainty introduced by using wt07 as reference has been estimated to be 0.16[5] $ms^{-1}$ for wind speeds below 11 $ms^{-1}$. Due to lack of reliable wind directional measurements from mast M2, it was decided to use the yaw position of wind turbine wt07 as reference wind direction for the western sector. The uncertainty of wind vane measurements is estimated to be larger than 5° caused by the large distance between mast M2 and the wind farm (2-6 km). Using the wind turbine wt07 yaw position as a reference, results in an uncertainty of more than 7° because the yaw misalignment also need to be included.

## 2.4 Atmospheric conditions

Since wake losses are highly dependent on the local meteorological conditions, an overview of the measurement setup is required. The analysis presented later will both refer to hub height and the low level measurements applicable for the stability classification.

### 2.4.1 Wind speed and direction

The wind climate was measured on M2 before the wind farm installation and reported in [11]. The mean wind speed at 62 m level was 9.5 $ms^{-1}$ during the initial period. Figure 3a shows the wind speed distribution representing the three year period from 15 May-1999-14 May 2002 of wind speed from mast M2 at 15 m height. The parameters of the Weibull distribution are similar to the distribution shown in Figure 3b; which represent three years of wind speeds measured from mast M7, height 20 m for the period of 1 Jan 2005-31 Dec 2007. Comparing Figure 3a and 3b concludes that the mean wind speed at 20 m level on M7 is unaffected by the wind farm wake. The wind rose in Figure 3c & 3d show that the wind direction in both periods is dominated by westerly winds. The distribution of wind direction is consistent between the two periods with minor differences being attributed to natural variability e.g. the increase in northwesterly winds in the later period.

### 2.4.2 Turbulence intensity

The turbulence intensity in this analysis is defined as the ratio between the standard deviation of the horizontal wind speed and the mean horizontal wind speed for a 10 minute period.

---

[5] The estimated uncertainty includes a contribution from the cup calibration, 0.10 m/s (class 1), power transducer 0.04 m/s and power curve verification 0.12 m/s.

The mean offshore turbulence intensity, as function of wind speed below hub height has been determined for the main flow sectors prior to the wind farm installation as shown in Figure 4a. The standard deviation at low wind speed is approximately 3% decreasing to 1.5% for each of the 4 sectors in Figure 4a. Figure 4b shows the mean offshore turbulence intensity at hub height for three eastern flow sectors. The standard deviation of the turbulence intensity in Figure 4b for the eastern sector (45-135°) is 6.4±2% at 10 $ms^{-1}$. Thus the variations by direction sector or period are not significant in comparison to the variability of turbulence intensity at each wind speed. Figure 4c shows the mean offshore turbulence intensity at 20 m height for the four principal flow sectors. The turbulence intensity at hub height, measured both prior to and after the installation of the wind farm illustrates conditions expected for offshore with increased turbulence intensity level for increasing wind speed above 10-15 $ms^{-1}$. This follows similar results for other offshore sites with highest turbulence intensities at low wind speeds, decreasing to a minimum around 8-12 $ms^{-1}$ and then increasing (e.g. [8]). Figure 4c shows a 2% increase in the turbulence intensity for a western [wake] sector (270±45°) for wind speeds below the rated wind speed compared to the other sectors. While the mean wind speed at 20 m height (10 m below tip-bottom height) is unaffected by the wind farm wake, the turbulence intensity is increased, which corresponds well to the preliminary studies [4] from Horns Rev wind farm. The variability of the turbulence intensities measured 20 m above mean sea level are unaffected by the wind farm wake except for very low wind speeds (~5 $ms^{-1}$).

### 2.4.3 Stability

The flow conditions expressed in term of an atmospheric stability classification has been established with reference to the Bulk Richardson approach. The Bulk Richardson number has been used as a stability parameters in many atmospheric studies (e.g. [13], [14]). The Bulk Richardson number ($R_{ib}$) is based on [15] from a single wind speed observation ($U_h$), measured at 15 - 20 m height (*h*) above mean sea level combined with the air and water temperature difference (Δt) from (eq. 1) and the absolute temperature (*T*) measured 13-16 m above mean sea level. The lowest possible recording height is chosen to minimize the wake effect on the measured wind speed.

$$Ri_b = -9.81 \times (\Delta t / \Delta h - 0.01) / (T \times (U_h / h)^2) \qquad \text{[eq. 1]}$$

The Obukhov length, L is derived from the $Ri_b$ number using equations 2 & 3. The objective is to provide a quantitative classification for atmospheric stability that can be used to examine

wake development. There are several methods for 'converting' the Bulk Richardson number to a Monin-Obukhov length (e.g. [13], [16]), The approach used here is based on [15]. The classification of the atmospheric stability is performed according to the definitions given in Table 1, which has been adopted from [17].

$$z / L = 10 \times Ri_b \qquad \text{for unstable stratification} \qquad \text{[eq. 2]}$$

$$z / L = \frac{10 \times Ri_b}{1 - 5 \times Ri_b} \qquad \text{for stable stratification} \qquad \text{[eq. 3]}$$

As mentioned in section 2.1 the time period overlap between mast M2 and M6/M7 measurements is limited. A direct comparison of the stability classifications shows minor discrepancies between the M2, M6 & M7 based classification, both for the "free" and "wake" sector observations in Figure 5. This investigation has been based on approximately 10,000 hours of measurements, corresponding to 3 years. A site classification of the frequency of occurrence of different stability classes is performed by direction classes for two wind speed intervals 5-10 $ms^{-1}$ and 10-15 $ms^{-1}$ - before and after installation of the wind farm as shown in Figure 6. As discussed in [6] the use of the air-water temperature difference to define stability classes tends to limit the number of observations in the near-neutral class. A further issue at Horns Rev is that temperatures are measured to a precision of 0.1 ºC. At moderate temperatures and at moderate/high wind speeds this inaccuracy will lead to minor differences (e.g. observations being placed in the very stable class rather than the stable class). However when temperature differences are small, the measurement precision could lead to erroneous classification. Hence the neutral and near-neutral classes (cL=-1, 0, 1) should be seen as a broad grouping. As shown in Figure 6, the frequency of stability classes is broadly similar for the two periods, with very minor differences at high wind speeds. The difference in the classification performed by the M2 and the M7 measurements is caused by the quality of the measuring equipment and the different periods as indicated in the comparison on Figure 5. For the 5-10 $ms^{-1}$ grouping, the frequency of stable conditions tends to be higher and the number of observations classified as near-neutral is lower in the second period (2005-2007). All time periods and wind speeds show a similar distribution of stability classes by direction with a larger number of near-neutral and unstable classes from the south and west and higher numbers of stable conditions from the east and south. This is broadly in line with the

distribution of stability classes at a number of Danish sites shown in [6]. Approximately 18% of the periods representing the wind speed range 5 – 15 $ms^{-1}$ are categorized as stable or very stable according to the distributions showed in Figure 6.

### 2.4.4 Turbulence intensity and atmospheric stability classification

Combining the turbulence intensity and the stability classification enables a determination of the turbulence intensity as function of wind speed that can be grouped according to the stability classification from the previous section. The relationship between turbulence intensity and atmospheric stability for three distinct wind speeds (5, 10 & 15 $ms^{-1}$) is shown in Figure 7a. The measurements were recorded at HR-M6, h=70m for an easterly flow sector. Figure 7a shows almost constant turbulence intensity for the stability classes cL≤1, furthermore a large part of the observations (>50%) occurs during unstable situations. Due to this observation, later analysis will be limited to only three stability groups (cL ≤ 1, cL=2 and cL=3). The relationship between turbulence intensity and atmospheric stability for the easterly sector are shown in Figure 7b and 7c for the two time periods and for the westerly sector in Figure 7d. The standard deviation is included as error bars in Figure 7. The classification decreased the variability of the turbulence intensity at 10 $ms^{-1}$ from 2.4% to 1.8% for the eastern sector in Figure 7b. For directions 0-180º the results for the two periods are similar for all three stability groups. As shown, turbulence intensity tends to be higher in unstable conditions (around 7%), than in stable conditions (4-5%). For the western sector (180-360º) results are shown for the pre-wind farm construction period only. Turbulence intensity shows the same distinct relationship to the stability groups as for the easterly directions. For example, at 10 $ms^{-1}$, turbulence intensity is close to 4% in the very stable class and 7% for the cL ≥ -1 stability group. The analysis illustrates that while atmospheric stability can broadly represent levels of atmospheric turbulence, this relationship is wind speed dependent. Conversely, a range of atmospheric stabilities can exist for different turbulence intensity levels in the atmosphere. As shown, the standard deviation for the neutral to very unstable class is similar to those of the stable and very stable classes.

# 3 Flow characterization

Previous flow analysis for wakes has been based on the power ratio, defined as the ratio between the power from the turbine operating in a wake and the wind turbine with free stream

undisturbed inflow (e.g. [17]. During the recent analysis, performed in UpWind, it was decided to reformulate and use the power deficit ($\eta_p$) defined with reference to the power ratio in eq. 4,

$$\eta_p = \left[1 - P_{wake} / P_{free}\right] \qquad \text{[eq. 4]}$$

The power deficit, $\eta_p$ ranges between 0 and 1 where $\eta_p$=0 indicates that the production from the wind turbine located [partly] in the wake is unaffected. Hence power deficit is inversely proportional to turbine or wind farm efficiency; an efficiency of 100% is equal to a power deficit of 0. The deficit is determined as function of flow direction, based on 10 minute power values for two neighboring wind turbines (e.g. wt07 & wt17). The power values are filtered to exclude periods if either of the turbines were partly or fully offline (e.g. start or stop sequences). Due to a lack of nearby reliable wind speed signal, the power value from the free stream wind turbine is used, with reference to the power curve in Figure 2a, to define the wind speed interval. In the following sections, the flow deficit is determined on three different levels 1) interaction between two neighboring wind turbines; 2) flow along a row of turbines and 3) for different atmospheric conditions.

## 3.1 Flow interaction between two wind turbines

The power deficit values were averaged using a 5 degree moving window technique as function of the wind direction for two wind turbines with spacing of 7 D. The mean deficit values as function of the normalized wind direction are shown in Figure 8a together with error bars representing the standard deviation. The mean standard deviation of the deficit is 0.10, but ranges between 0.06 – 0.17. A quantification of the power deficit is difficult due to scatter in the results, often caused by lack of observations in a particular wind speed range or a directional sector. Assuming that the power deficit distribution can be skew and asymmetric, it has been necessary to implement a robust expression to extract information about the distribution properties such as the maximum wake deficit and the size of the wake expansion.

The power deficit distribution can be fitted with an expression as function of wind direction ($\theta$):

$$f(\theta) = a_0 + (a_1 + a_2 \times \theta + a_3 \times \theta^2) \times \exp(-a_4 \times \theta^2) \qquad \text{[eq.5]}$$

Where the variables $a_0$, $a_1$, $a_2$, $a_3$ and $a_4$ are determined by fitting eq. 5 to the mean deficit values, as function of the normalized wind direction $\theta$. The fitted distribution $f(\theta)$ is shown in

Figure 8a representing the wind speed range 7-9 $ms^{-1}$. This distribution is characterized with a maximum deficit of 0.41 and a wake expansion of 28 degrees. The wake expansion width is defined as the 95% confidence level with reference to the fitted power deficit distribution $f(\theta)$. For this wind speed range, the standard deviation of the maximum deficit is 0.41±0.14, but both the maximum deficit and the standard deviation depend on the size of the moving window. Decreasing the size of the moving window below 5° introduces more scatter in the deficit distribution for the Horns Rev dataset, furthermore using a wind directional reference based on the wind turbine yaw position contributes to this scatter.

The basic wake characteristics of the wind turbine are summarized in Table 2. The table presents both maximum deficit and the wake expansion for the wind speed range 3 – 13 $ms^{-1}$ for 2 $ms^{-1}$ wind speed bins. The constant maximum deficit for the wind speed range 5 - 9 $ms^{-1}$ reflects the constant thrust coefficient in this range as shown in Figure 2a. The wake expansion also seems to be dependent on thrust coefficient with wider wakes in the lowest wind speed bins.

## 3.2 Power deficit as function of stability

The maximum power deficit and the wake expansion, presented in Table 2 depend on the ambient turbulence intensity, atmospheric stability and the wind turbine thrust coefficient. The wind turbine thrust depends on the wind speed as shown in Figure 2a, but also on the rotor speed and the pitch angle setting, shown in Figure 2b.

Figure 8b displays the power deficit distribution for three distinct groups of stability characterized with cL=3, cL=2 and cL≤1. The figure demonstrates a strong correlation with the atmospheric stability and how the wake is wider and deeper during very stable conditions (cL=3), caused by decreased turbulent mixing of the wake. Note that while the wake is wider in the stable case (cL=2) the maximum power deficit at the center of the wake is slightly less than for the remaining near-neutral and unstable cases (cL<2). The turbulence intensity is broadly similar for all stability classes except for stable and very stable conditions according the current analysis (Figure 7).

The large amount of available data enables a determination of the power deficit as function of turbulence intensity for a large range of turbulence intensities based on data representing a wind speed range 6 – 12 $ms^{-1}$. Figure 8c illustrates an almost linear relation between the

maximum power deficit and the ambient turbulence intensity for two different spacing 7 D and 10.4 D. Figure 8c furthermore shows that increased wind turbine spacing from 7 D to 10.4 D, decreases the power deficit level by about 33%. The variability in terms of standard deviation of the maximum power deficit values is approximately constant with increasing turbulence intensity (~0.1) and has been included in Figure 8c.

As shown in this section, there are strong relationships between a number of atmospheric variables that are linked by a complex relationship between wind speed, turbulence intensity and atmospheric stability. This means that the power deficit at any wind farm is likely to vary by direction not just as a result of different turbine spacing but also because the wind speed distribution, atmospheric stability and turbulence intensity vary by direction. In the following section, the power deficit at Horns Rev is examined to assess whether these relationships can be determined even within a large wind farm where the turbulence intensity is not solely dependent on ambient conditions but also on turbine generated turbulence intensity [19].

## 3.3 Power deficit along rows of wind turbines

This analysis was initiated from previous analysis used for model evaluation as part of the UpWind project, where a large number of flow cases were formulated without taking into account the atmospheric stability information [18]. The power deficit along a row of turbines has been determined for four flow cases with spacing of 7 D, 9.4 D, 10.4 D and >20 D respectively and an inflow sector of 30 degrees; which is applicable for the engineering models like WAsP® [20].

Before the measurements can be analyzed, a number of filtering criteria have been formulated and implemented:

i) Reference wind turbine wt07 is grid connected 100%,

ii) Object wind turbine is grid connected 100%,

iii) All wake generating wind turbines are grid connected 100%

iv) Flow stationarity throughout the whole wind farm. This clause eliminates many observations when analyzing narrow flow sectors (≤5°) and only needs to be included for large wind farms (L≥2 km).

Clause iv) concerning flow stationarity is used to exclude periods, where the wind farm is partly covered by weather fronts. The clause is positive when two consecutive observations belongs to the same flow case e.g. $7.5 < V_{hub} \leq 8.5$ ms$^{-1}$ and $255° < Wdir \leq 285º$ and then the second of two consecutive observations is included.

The mean flow deficit for four turbine spacing's (7, 9.4, 10.4 and >20 D) are shown in Figure 9a and 9b as function of spacing distance, except (>20 D) which is presented as function of 7D spacing distance. The level of the power deficit depends on the sector size, wind turbine thrust and the atmospheric stability. Note that because the power deficit at the boundary turbines differs from the deficit inside the wind farm the power deficit from the edge or boundary turbines were omitted from the present analysis[6]. The Figure demonstrates how the power deficit increases inside the wind farm towards 0.35 – 0.40 for a wind speed range of 7.5 - 8.5 ms$^{-1}$. Each deficit curve represents a 30 degree flow sector, centered on the direction for a given turbine spacing. Flow from 244º has a large spacing (>20 D) due to the geometrical wind farm layout. The deficit from this direction increases more slowly than for the closer turbine spacing, (Figure 9a; Wdir=244°) and reaches the deficit level for the other spacing at 24 D. The standard deviation of the power deficit values is 0.15 - 0.20 and included as error bars on both Figure 9a and 9b. Each deficit curve is based on more than 100 hours of operation.

Decreasing the size of the flow direction sector will result in a faster increase in the power deficit due to the focusing of the analysis closer to the wake center and the approximately Gaussian nature of the power deficit curve (Figure 8a and 8 b). 7 D spacing combined with a ±2.5° flow sector will result in a deficit of 0.4 approximately 7 D behind the free stream wind turbine as shown in Figure 8a and this deficit level is almost constant through the wind farm.

## 3.4 Power deficit for different spacing

Given that one of the major questions in wind farm design is 'What is the optimal spacing for wind turbines?' the analysis above was repeated using two different directions that give larger spacing and also to assess whether differences could be discerned for the different stability classes. The preliminary flow sector size is ±15º, corresponding to the previous flow cases in

[6] The results for 7 D and 24D spacing includes deficits for wind turbines located in rows 2-7 (=W→E *direction) and the diagonals (9.4 D and 10.4 D) include rows consisting of 7 turbines.

Figure 9, in order to classify the results into three distinct groups of stability introduced previously in section 3.2. This introduces some uncertainty because the average wind speed in each stability class varies. Nonetheless it is an evaluation of how consistent the relationships between the power deficit with both atmospheric stability and spacing. Results are shown in Figure 10a, 10b, 10c and 10d where each figure presents the averaged deficit as function of spacing distance, except (>20 D) which is presented as function of 7D spacing distance. The variability of the power deficit values, is approximately 0.2 except for very stable conditions and 7D spacing, where standard deviation increases to 0.3. Decreasing the flow sector towards ±2.5º still results in a standard deviation of 0.2. The deficit for large spacing >20 D in Figure 10b is not sensitive to the stability while decreasing spacing results in increased sensitivity. The very stable class shows a power deficit that is initially larger and continues to increase deep inside the wind farm. For the neutral to unstable classes the power deficit is initially smaller and remains lower through the wind farm. The remaining classes fall between these results but with some variability that can be ascribed to wind speed variations. Figure 10a, 10c & 10d illustrates the deficit for three different wind turbine spacing: 7 D, 9.4 D & 10.4 D. The largest deficits occur during stable and very stable conditions, while the deficit shows very similar behavior during all other conditions. It can also be seen that the differences between 9.4 D and 10.4 D are very small whereas the initial power deficits at 7 D are noticeably larger. Figure 10 represents 280 hours of the production time in the wind speed range 7.5 – 8.5 $ms^{-1}$. The wind farm efficiency is defined as a summation of the individual wind turbine production - with reference to wt07. The wind farm efficiency, corresponding to the 4 x 3 flow cases presented in Figure 10, varies between 0.71 – 0.84, where 0.71 represents a 7 D spacing, 30° flow sector and wind speed range 8±0.5 $ms^{-1}$. Decreasing the 7 D spacing flow sector to 5° will reduce the park efficiency to 0.66; This small flow sector is less frequent, but still important for model validation as shown in [21,22].

## 4 Conclusions

The mean power deficit depends on the mean wind speed, wind turbine spacing, turbulence intensity and the stability conditions as demonstrated in the analysis of Horns Rev measurements. Our analysis shows general tendencies in the relationship between power deficits, wind speed turbulence and stability yet it must be acknowledged that the variability

within each class (as indicated by the standard deviation) is typically larger than the differences between classes.

As shown, relationships between wind speed, turbulence intensity and atmospheric stability offshore are complex. There is also a strong relationship between the wind direction and the atmospheric variables that influences the power deficit/wake width in addition to the turbine spacing.

Classification of the stability condition for the Horns Rev offshore wind farm has been established based on the Bulk-Ri method. The site stability classification for Horns Rev was determined for the wind turbine operational wind speed interval 5 – 15 $ms^{-1}$. Results from the data analysis performed as part of the UpWind project were combined with data on stability conditions to investigate the wind turbine power deficit in different stability conditions.

Analysis of the measurements from Horns Rev shows a distinct correlation between the stability conditions and the turbulence intensity. Very stable conditions results in low average turbulence intensities of 4%. Turbulence intensity levels tend to increase as atmospheric conditions become more unstable. On average, however, lowest turbulence intensities are experienced between 8 and 12 $ms^{-1}$ when wake losses are high due to a relatively high turbine thrust coefficient.

Detailed analysis of the power deficit between two neighboring wind turbines with a spacing of 7 D reveals the angular power deficit distribution with a maximum of 0.41 and a angular width 25 degrees. Characterization of the power deficit inside Horns Rev wind farm shows that each wind turbine generates a power deficit sector of 25-35 degrees, where sector size and the maximum power deficit depend on the stability conditions. The analysis also demonstrates a distinct near-linear relationship between maximum power deficit and the turbulence intensity where the level and slope highly depends on the wind turbine spacing.

The mean power deficit along single wind turbine rows is similar in the wind speed interval from 6 to 10 $ms^{-1}$ and for the same inflow direction, but the maximum deficit decreases with increasing wind speed. The largest power deficit occurs between first and the second wind turbine while the remaining downstream power deficit is small. The mean power deficit for other inflow sectors increases more slowly downstream - compared to the previous flow sector and the resulting power deficit in the far end of the wind farm decreases slightly.

The final power deficit analysis combined with stability conditions demonstrates that very stable or stable conditions results in larger mean power deficits, while there is little difference in the mean power deficits for the other stability conditions (near-neutral and the unstable classes).

## Acknowledgements

Research funded in part by EU project UpWind # SES6 019945 and the National Science Foundation CBET-0828655/CBET-1067007. We would like to acknowledge and Vattenfall AB and DONG Energy A/S for data from the Horns Rev wind farm. Thanks also to the anonymous reviewers whose comments improved the clarity of the paper.

## References

1. Dahlberg JÅ and SE Thor. *Power performance and wake effects in the closely spaced Lillgrund offshore wind farm*. in *European Offshore Conference*. 2009. Stockholm.
2. Troldborg N, JN Sorensen and R Mikkelsen, *Numerical simulations of wake characteristics of a wind turbine in uniform in flow.* Wind Energy, 2010. **13**: 86-99.
3. Barthelmie RJ and LE Jensen, *Evaluation of power losses due to wind turbine wakes at the Nysted offshore wind farm.* Wind Energy, 2010. **13**: 573-586.
4. Jensen L. *Wake measurements from the Horns Rev wind farm*. in *European Wind Energy Conference*. 2004: EWEA (on CD).
5. Jensen LE. *Array efficiency at Horns Rev and the effect of atmospheric stability*. in *European Wind Energy Conference*. 2007.
6. Motta M, RJ Barthelmie and P Vølund, *The influence of non-logarithmic wind speed profiles on potential power output at Danish offshore sites.* Wind Energy, 2005. **8**: 219-236.
7. Van Wijk AJM, ACM Beljaars, AAM Holtslag and WC Turkenburg, *Evaluation of stability corrections in wind speed profiles over the North Sea.* Journal of Wind Engineering and Industrial Aerodynamics, 1990. **33**: 551-566.
8. Türk M and S Emeis, *The dependence of offshore turbulence intensity on wind speed* Journal of Wind Engineering and Industrial Aerodynamics, 2010. **98**(8-9): 466-471.
9. Barthelmie R, O Hansen, K Enevoldsen, J Højstrup, S Larsen, S Frandsen, S Pryor, M Motta and P Sanderhoff, *Ten years of meteorological measurements for offshore wind farms.* Journal of Solar Energy Engineering, 2005. **127(2)**: 170-176.
10. Sommer A and KS Hansen, *Wind Resources at Horns Rev*. 2002, Tech-wise:Eltra PSO-2000 Proj. nr. EG-05 3248. DK-7000 Fredericia. p. 89. http://130.226.56.153/rispubl/NEI/nei-dk-4851.pdf.
11. Sørensen PB and KS Hansen, *Wake effect east of the Horns Rev offshore wind farm*. 2002, Elkraft System:PSO-F&U 2002/FU 2103. DK-7000 Fredericia. p. Available on request.
12. Réthoré PE, NA Johansen, ST Frandsen, RJ Barthelmie, KS Hansen, LE Jensen, MAB Bækgaard and JR Kristoffersen. *Systematic wind farm measurement data reinforcement tool for wake model calibration*. in *European Offshore Wind Conference*. 2009. Stockholm, Spetember 2009 http://www.iop.org/EJ/article/-search=56576984.2/1742-6596/75/1/012047/jpconf7_75_012047.pdf?request-id=e6fd0138-b514-4c09-a647-5d03e6b72bf9.
13. Hsu SA, *The relationship between the Monin-Obukhov stability parameter and the bulk Richardson number at sea.* Journal of Geophysical Research, 1989. **94**(C6): 8053-8054.
14. Zoumakis NM and AG Kelessis, *The dependence of the bulk Richardson number on stability in the surface layer.* Boundary-Layer Meteorology, 1991. **57**(4): 407.

15. Grachev AA and CW Fairall, *Dependence of the Monin-Obukhov stability parameter on the bulk Richardson number over the ocean.* Journal of Applied Meteorology, 1995. **36**: 406-414.

16. Large WG and S Pond, *Sensible and latent heat flux measurements over the ocean*. Journal of Physical Oceanography, 1982. **12 464-482**.

17. Hasager C, A Peña, T Mikkelsen, S-E Gryning, M Courtney, PB Sørensen, *12MW: Final report*, Report number Risø-R-1690(EN) June 2009.

18. Barthelmie RJ, SC Pryor, ST Frandsen, K Hansen, JG Schepers, K Rados, W Schlez, A Neubert, LE Jensen and S Neckelmann, *Quantifying the impact of wind turbine wakes on power output at offshore wind farms*. Journal of Atmospheric and Oceanic Technology, 2010. **27**(8): 1302-1317.

19. Frandsen S and ML Thøgersen, *Integrated fatigue loading for wind turbines in wind farms by combining ambient turbulence and wakes.* Wind Engineering, 1999. **23**: 327-339.

20. Mortensen NG, DN Heathfield, L Myllerup, L Landberg and O Rathmann (2005) *Wind Atlas Analysis and Application Program: WAsP 8 Help Facility*. Risø National Laboratory, Roskilde, Denmark. 335 topics. ISBN 87-550-3457-8, http://www.risoe.dk/vea/projects/nimo/WAsPHelp/Wasp8.htm.

21. Barthelmie RJ,KS Hansen, ST Frandsen, O Rathmann, JG Schepers, W Schlez, J Phillips, K Rados, A Zervos, ES Politis and PK Chaviaropoulos, *Modelling and Measuring Flow and Wind Turbine Wakes in Large Wind Farms Offshore.* Wind Energy, 2009. **12:** 431-444.

22. Ivanell S, R Mikkelsen, JN Sørensen, KS Hansen and D Henningson, *The impact of wind direction in atmospheric BL on interacting wakes at Horns Rev wind farm. Presented The science of making torque from wind* presented at Torque, 2010, Crete, June 2010. http://orbit.dtu.dk/getResource?recordId=274359&objectId=1&versionId=1

Table1: Atmospheric stability classes according to intervals of the Obukhov length.

| Class | Obukhov length [m] | Atmospheric stability class |
|---|---|---|
| **cL=-3** | -100 ≤ L ≤ -50 | Very unstable (vu) |
| **cL=-2** | -200 ≤ L ≤ -100 | Unstable (u) |
| **cL=-1** | -500 ≤ L ≤ -200 | Near unstable (nu) |
| **cL=0** | \|L\|>500 | Neutral (n) |
| **cL=1** | 200 ≤ L ≤ 500 | Near stable (ns) |
| **cL=2** | 50 ≤ L ≤ 200 | Stable (s) |
| **cL=3** | 10 ≤ L ≤ 50 | Very stable (vs) |

Table 2: Maximum power deficit and wake expansion for 5 wind speed ranges representing 7D wind turbine spacing at Horns Rev.
The wind speed is measured at wind turbine hub height.

| Wind speed range | maximum deficit | wake expansion - [°] |
|---|---|---|
| 3 - 5 $ms^{-1}$ | 0.50 | 29 |
| 5 - 7 $ms^{-1}$ | 0.41 | 30 |
| 7 - 9 $ms^{-1}$ | 0.41 | 28 |
| 9 - 11 $ms^{-1}$ | 0.36 | 25 |
| 11 - 13 $ms^{-1}$ | 0.31 | 25 |

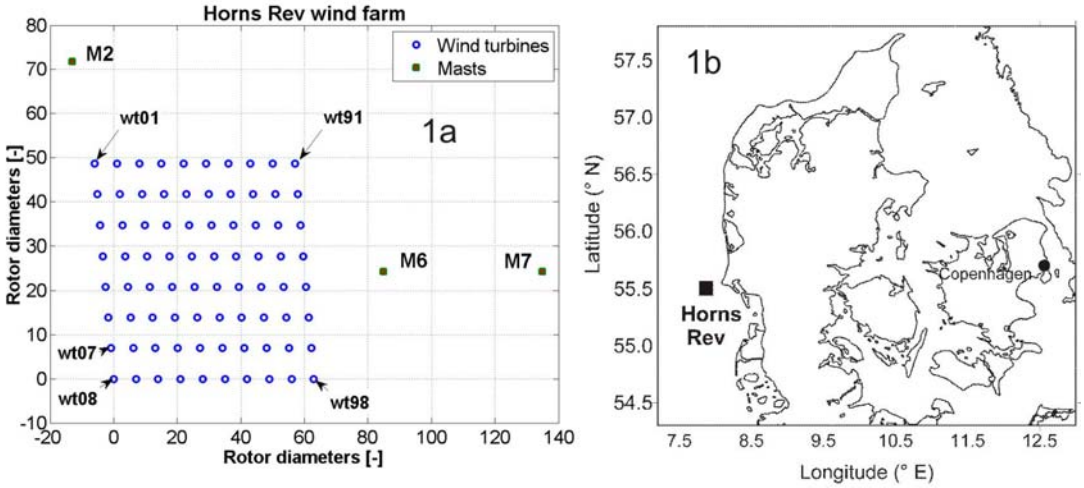


Figure 1: Location and layout of Horns Rev wind farm
including three nearby off shore masts (M2, M6 & M7).

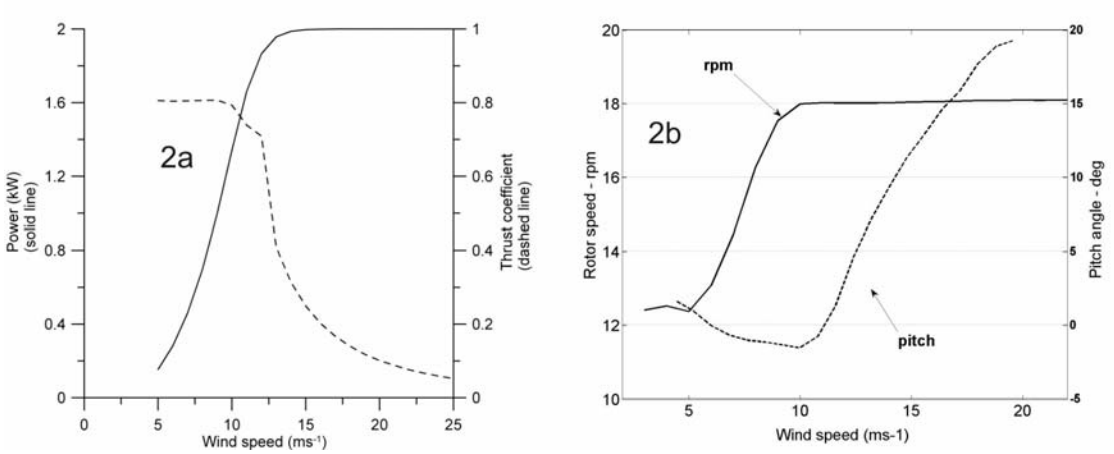


Figure 2: 2a shows the power (P) curve and thrust ($C_T$) coefficient curve for the VESTAS V80 turbine. 2b shows the averaged rotor speed and the average pitch angle both as function of wind speed at hub height.

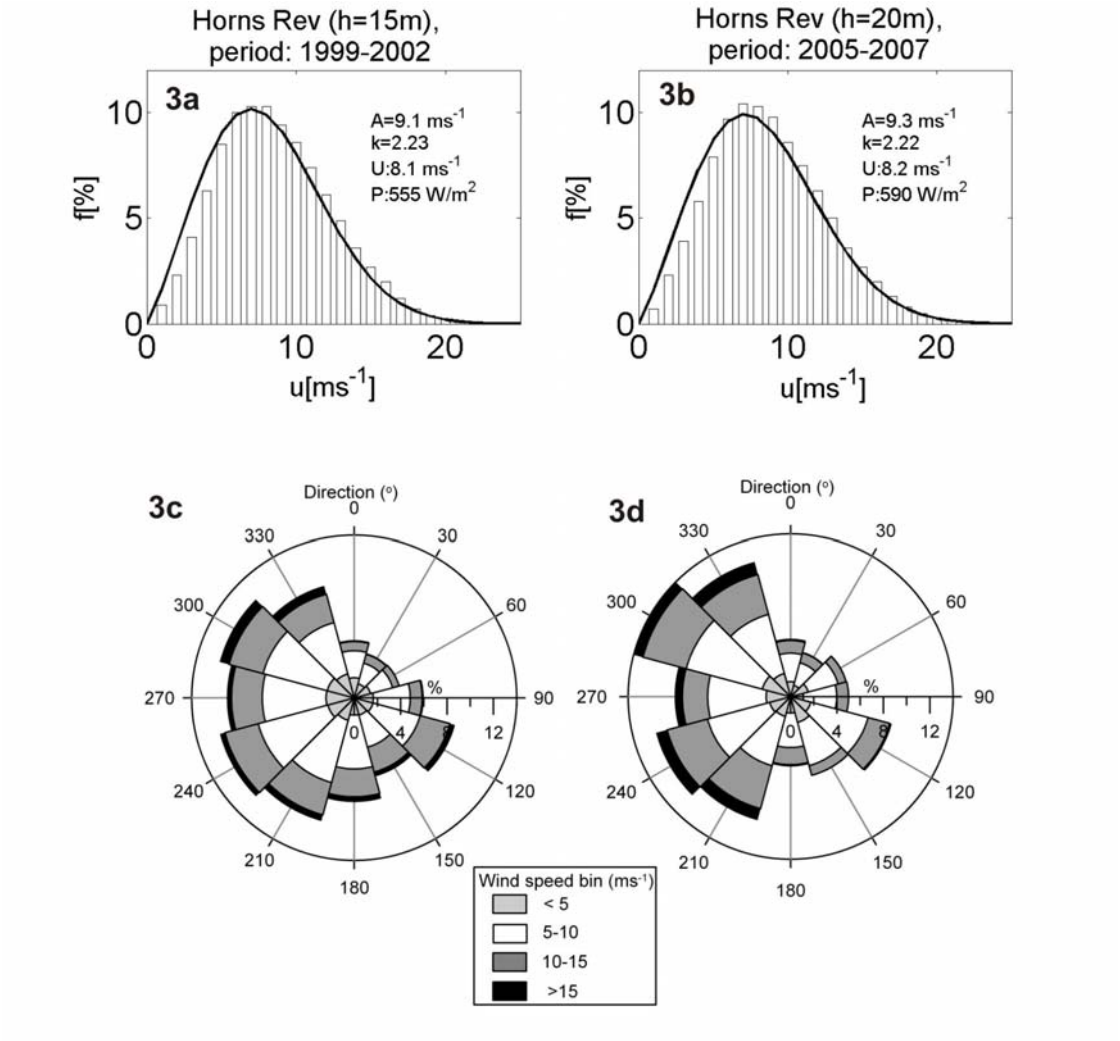


Figure 3: Wind speed distributions and wind roses for Horns Rev. Figure 3a shows the Weibull distribution from data measured before the wind farm installation in the period 15.05.1999-14.05.2002 and Figure 3b shows the Weibull distribution from data measured during the wind farm monitoring period 01.01.2005-31.12.2007. Figure 3c shows the wind direction distribution from the earlier period and Figure 3d shows the wind direction from the later period (corresponding periods to Figure 3a and 3b respectively)

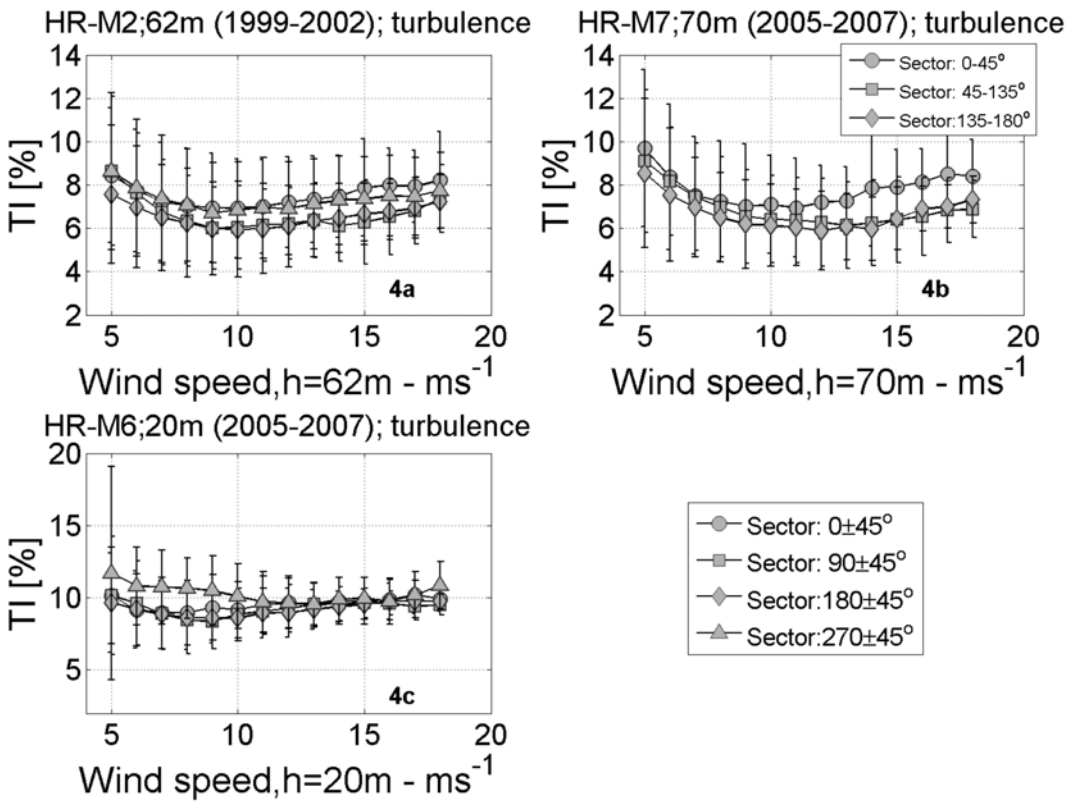


Figure 4: Three years of mean turbulence intensities shown by direction sector including one standard deviation. Figure 4a shows turbulence intensity measured before the wind farm installation at 62 m on mast M2 recorded in 15.5.1999-14.5.2002. The standard deviation of the turbulence intensity decreases from 3% to 1.5% for increasing wind speed. Figure 4b shows turbulence intensity measured during the wind farm monitoring period on mast M6 at 70 m during 01.01.2005-31.12.2007. Figure 4c presents 3 years of turbulence intensities from mast M6 at 20m height for the later period.

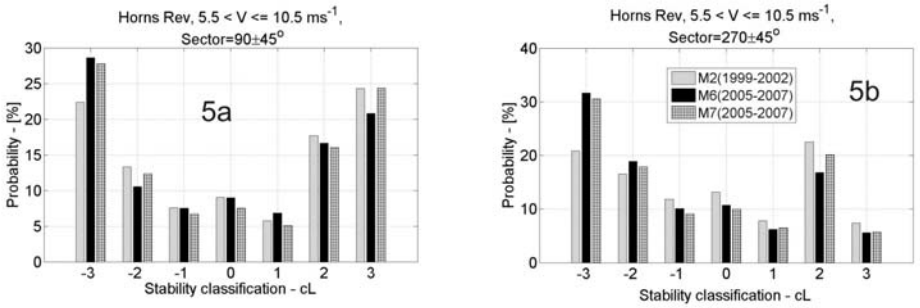


Figure 5: Figure 5a illustrates the free flow stability classification from an eastern direction and Figure 5b illustrates the wake flow classification for a western flow sector. The stability classification at Horns Rev is based on measurements from mast M2, M6 & M7. M2 measurements were recorded during 15.05.1999-14.05.2002 and M6 + M7 measurements represent 3 years (01.01.2005-31.12.2007) with an operating wind farm. Definitions of the stability classes are shown in Table 1.

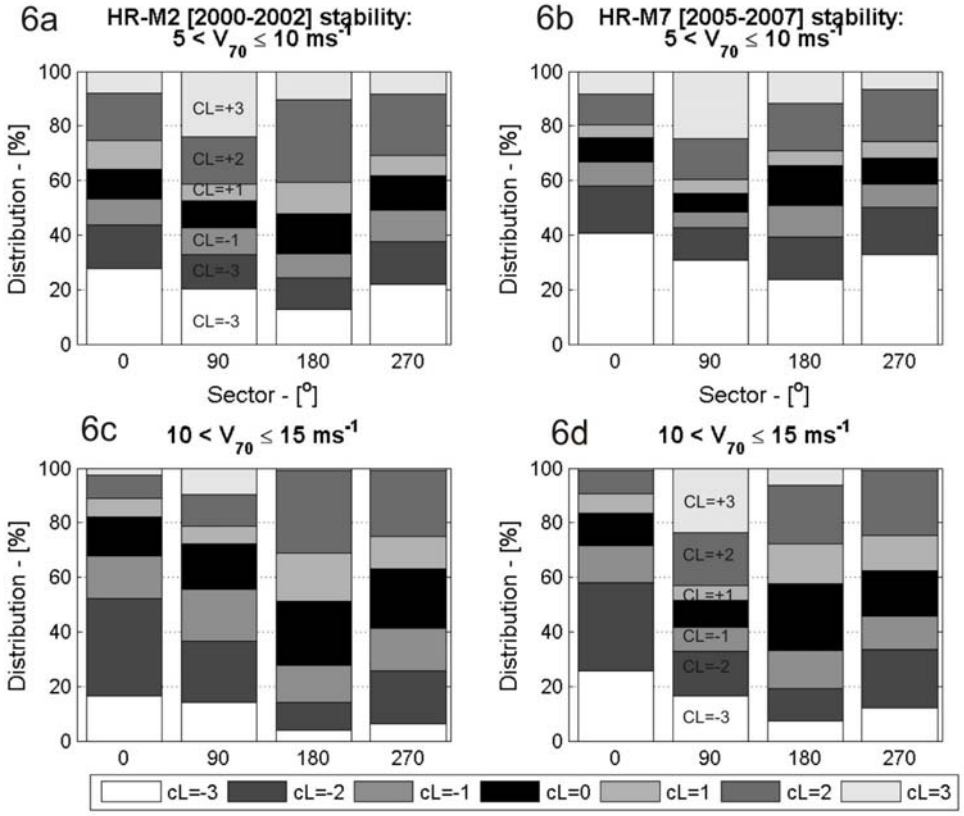


Figure 6: Observations divided into stability classes (shown in Table 1) in four direction sectors (0±45º, 90±45º, 180±45º and 270±45º). Figures 6a and 6c are derived from data measured before the wind farm installation (15.05.1999 – 14.05.2002) while figures 6b and 6d represents the wind farm monitoring period (01.01.2005 – 31.12.2007). The figures above (6a and 6b) show data selected from wind speeds between 5 and 10 $ms^{-1}$ while the figures below (6c and 6d) show data selected from wind speeds between 10 and 15 $ms^{-1}$.

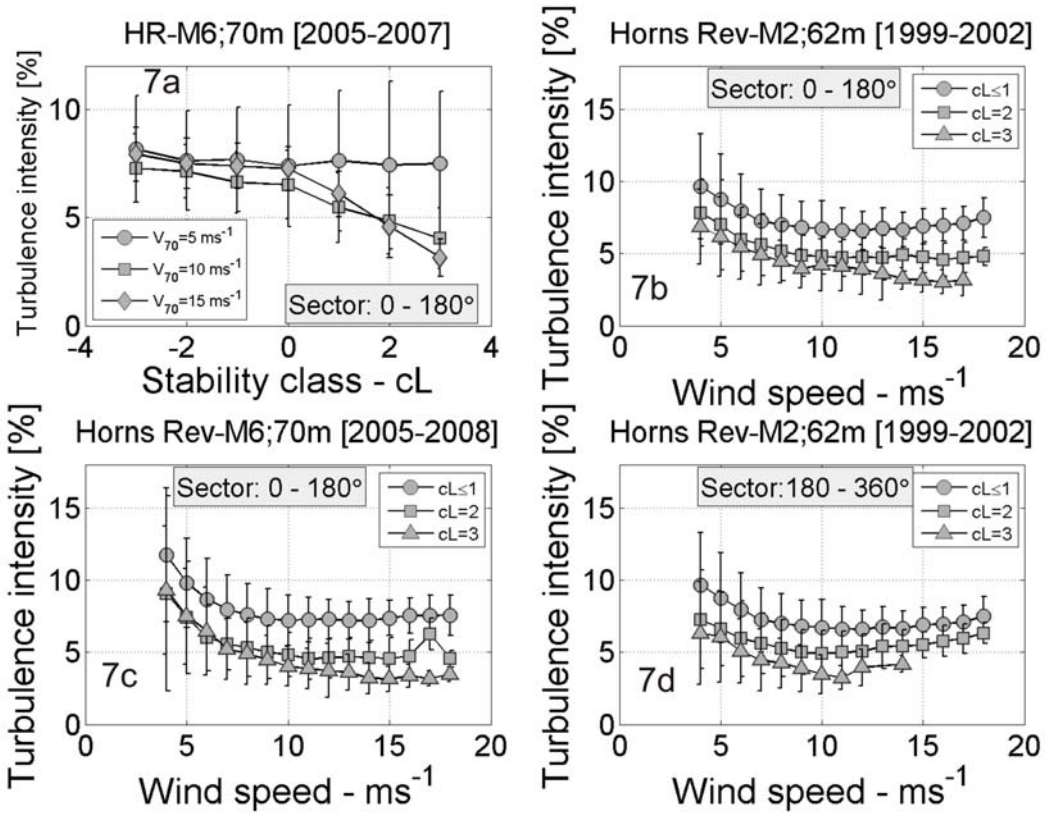


Figure 7: Three years of average turbulence intensity measurements for easterly and westerly wind - grouped by the stability classes. Figure 7a shows the mean turbulence for a three distinct wind speeds as function of stability classes where error bars represent one standard deviation. Figure 7b and 7d shows turbulence intensity measured before the wind farm installation (1999-2002) for the easterly and westerly sectors and 7c shows turbulence intensity during the wind farm monitoring period (2005-2007) for the easterly sector. Error bars representing one standard deviation for stability group cL ≤ 1, 2 & 3 have been included.

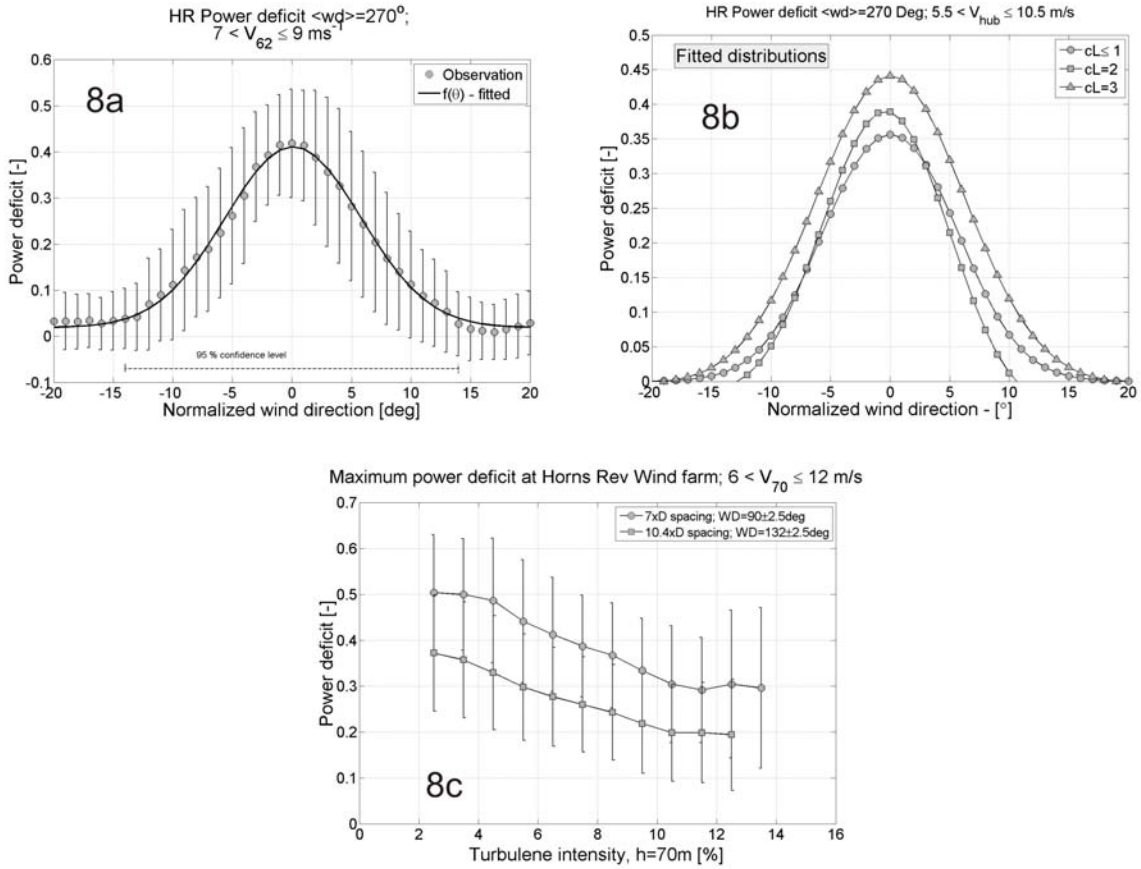


Figure 8: Power deficit at Horns Rev. Figure 8a shows the power deficit distribution as function of normalized wind direction for Horns Rev wind turbine wt17 compared to wt07 (spacing 7D). Turbine locations are shown in Figure 1. Wind speeds were selected with reference to M2 at 62 m for directions 270º in Figure 8a. One standard deviation representing each 5° sector has been included as error bars. Figure 8b shows fitted power deficit distributions for wt17 relative to wt07 - grouped on stability classes; cL=3, 2 & ≤1. Figure 8c shows the maximum power deficit for 7D and 10.4D spacing as function of turbulence intensity averaged for a 5° inflow sector. The wind speed interval 6 - 12 $ms^{-1}$ and turbulence intensity is measured at M6, 70m and the standard deviation has been included as error bars.

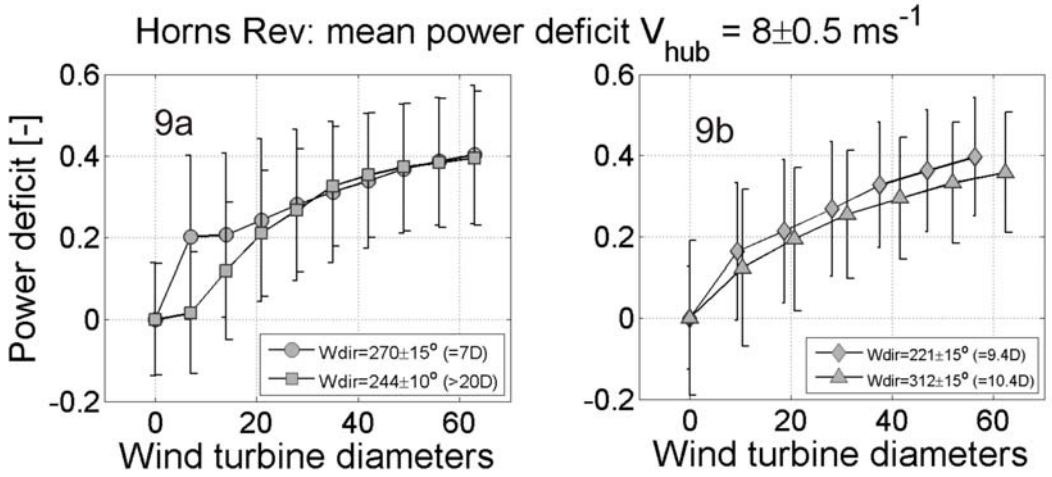


Figure 9: 9a and 9b shows the mean power deficits along rows of wind turbines for different spacing: 7D, 9.4D, 10.4D and >20D, where the curve represents a 30° flow sector except for 244°; which represents a 20° flow sector. The wind speeds range is 8±0.5ms-1. One standard deviation has been included as error bars.

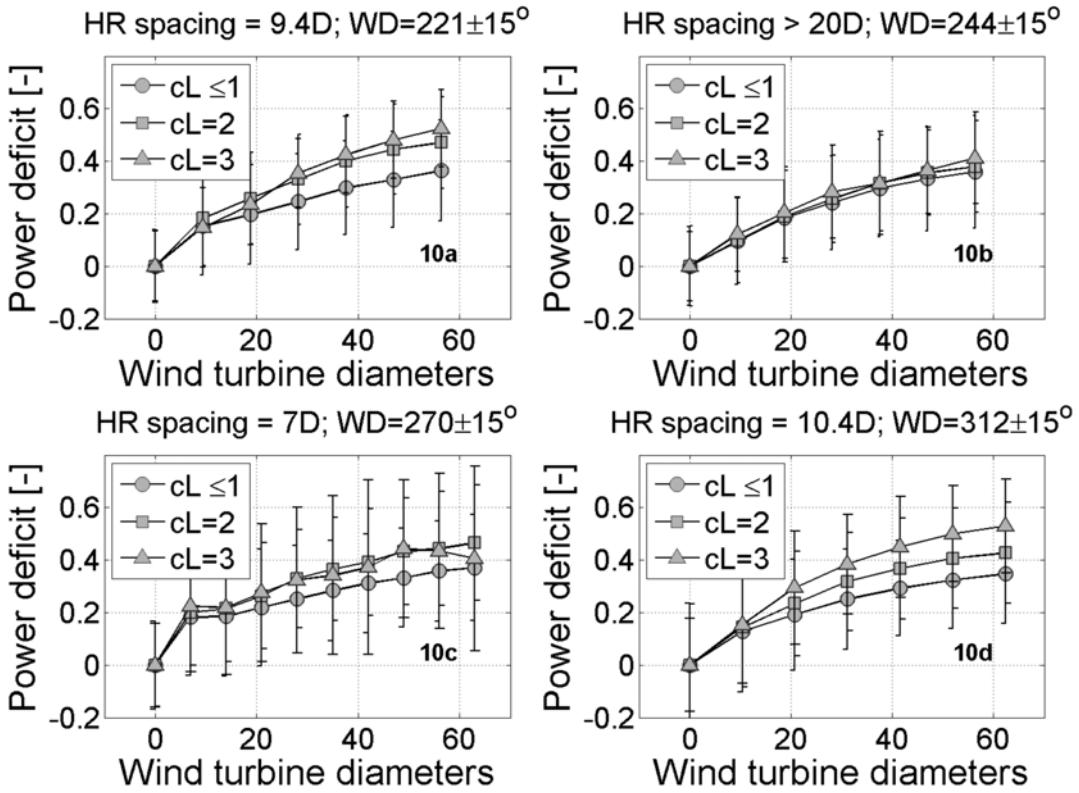


Figure 10: Horns Rev power deficit along rows with 7 – 10 turbines grouped by stability classes. Figure 10a represents 5 rows of turbines with a spacing of 9.4D selected by direction (221±15º), Figure 10b represents a large spacing (>20D) with direction 244±10°, Figure 10c represents 6 rows of turbines with a spacing of 7D for direction 270±15° and Figure 10d represents 5 rows of turbines with a spacing of 10.4D for direction 312±15°. The stability is grouped in very stable (cL=3), stable (cL=2) and other (cL≤1) stability classes and the wind speed range is 8.0±0.5 $ms^{-1}$. One standard deviation has been included as error bars.